

CRITICAL ANGLE IN THE PARTON CASCADE

Wolfgang Ochs

*Max-Planck-Institut für Physik, Werner Heisenberg Institut,
Föhringer Ring 6, D 80805 München, Germany*

Jacek Wosiek

*Institute of Physics, Jagellonian University,
PL 30-059 Cracow, Reymonta 4, Poland*

Abstract

The angular correlation function of partons in a jet as derived from perturbative QCD is nonanalytic at a critical angle which separates a multiparticle regime with scaling properties from a regime with few particles near the hadronisation scale. Some phenomenological consequences are discussed.

MPI-Ph/95-98

TPJU-17/95

November, 1995

hep-ph/9511457

arXiv:hep-ph/9511457v1 29 Nov 1995

I. INTRODUCTION

Recent studies of angular correlations of partons inside jets within perturbative QCD have demonstrated the emergence of scaling properties at high energies and at sufficiently large relative angles [1]- [5]. In this paper we focus on the complementary kinematic region of small relative angles within the same theoretical approach of perturbative QCD. The correlation function becomes nonanalytic in the high energy limit with a discontinuous second derivative for a critical angle ϑ_c which separates two regimes of quite different characteristics. In the small angle regime the correlation function is determined by the one-particle energy spectrum of the parent parton from which the detected partons emerge. In the theory with running α_s the correlation function in this new regime depends on the nonperturbative transverse momentum cutoff Q_0 in the cascade whereas in the large angle regime there was no cutoff dependence. This opens the possibility to test the hypothesis of “Local Parton Hadron Duality” (LPHD) [6] near the boundary Q_0 .

The occurrence of a critical angle ϑ_c in the angular correlation has been noted already in two previous papers. In our first study on angular correlations [2] we found (for fixed α_s) a relation between 2-particle correlations, and the 1-particle spectrum for the critical angle

$$\vartheta_c = \frac{Q_0}{P} \left(\frac{P\Theta}{Q_0} \right)^{1/5} \quad (1.1)$$

and also for correlations in a pair of points symmetric in certain variables around this critical angle (Θ and P are the opening angle and primary momenta of the jet respectively).

In the analysis by Dokshitzer, Marchesini and Oriani [1] the same angle (1.1) was found as limiting the validity of a power law in the relative angle from below (again for fixed α_s). Moreover they suggested the existence of a correlation function below ϑ_c in a nonperturbative model: the rate for the particles with relative angle ϑ_{12} is given in terms of the momentum distribution of the parents.

We show in the following that perturbative QCD in its regime of applicability, ie. for transverse momenta $k_T \geq Q_0$, provides the correlation function not only above but also

below ϑ_c . It can be expressed indeed by the momentum distribution of the parent parton in some analogy to the above effective hadronic model [1]. Furthermore we extend the analysis to the interesting case of running α_s . Again a critical angle can be identified. At high energies it behaves as

$$\vartheta_c = \frac{\Lambda}{P} \left(\frac{\ln(P\Theta/\Lambda)}{\lambda} \right)^{\frac{4}{9}\lambda} \quad (1.2)$$

which depends more weakly on the jet energy than the angle (1.1) for constant α_s (Λ is the QCD scale and $\lambda = \ln(Q_0/\Lambda)$). The special role of the critical angle as singular point becomes obvious from the fact that the correlation function depends on the cutoff Q_0 only below but not above it.

II. EMERGENCE OF THE CRITICAL ANGLE IN PERTURBATIVE QCD

We consider for definiteness the correlation density $\rho^{(2)}(\vartheta_{12}, P, \Theta)$ in the relative angle ϑ_{12} of two partons and comment later on multiparton correlations. In the double logarithmic approximation (DLA) the correlation function obeys the integral equation [3]

$$\rho^{(2)}(\vartheta_{12}, P, \Theta) = d^{(2)}(\vartheta_{12}, P, \Theta) + \int_{Q_0/\vartheta_{12}}^P \frac{dK}{K} \int_{\vartheta_{12}}^{\Theta} \frac{d\Psi}{\Psi} \gamma_0^2(K\Psi) \rho^{(2)}(\vartheta_{12}, K, \Psi). \quad (2.1)$$

where the anomalous dimension γ_0 for the evolution of the multiplicity is given in terms of the running coupling $\gamma_0^2 = 6\alpha_s/\pi = \beta^2/\ln(k_T/Q_0)$ with $\beta^2 = 12N_c/(11N_c - 2N_f)$. The inhomogenous term $d^{(2)}$ is constructed from the product of 1-particle angular distributions and found as $d^{(2)}(x) = \rho^{(1)}(x)\bar{n}(x)$, $x = P\vartheta_{12}/\Lambda$ and with the multiplicity \bar{n} in the cone of half-angle ϑ_{12} around the primary parton axis. In exponential accuracy $d^{(2)} \sim \bar{n}^2$.

The leading contribution to the solution of Eq.(2.1) was derived in [3]¹

$$\rho^{(2)}(\vartheta_{12}, \Theta, P) = \int_{Q_0/\vartheta_{12}}^P \frac{dK}{K} R \left(\frac{P}{K}, \frac{\Theta}{\vartheta_{12}}, \frac{K\vartheta_{12}}{\Lambda} \right) d^{(2)} \left(\frac{K\vartheta_{12}}{\Lambda} \right). \quad (2.2)$$

¹Present $R(P/K)$ denotes $\bar{R}(P/K) + \delta(1 - P/K)$ of Ref. [3].

The resolvent $R\left(\frac{P}{K}, \frac{\Theta}{\vartheta_{12}}, \frac{K\vartheta_{12}}{\Lambda}\right)$ is the momentum distribution of the parent partons K in the jet (P, Θ) with the condition, that their virtuality is bounded from below by $K\vartheta_{12}$ and *not* by the elementary cut-off Q_0 . This is equivalent to limiting from below their emission angle by ϑ_{12} . The representation (2.2), which was derived as the solution of the differential equation (2.1) is identical with the jet calculus result used in Ref. [1].

In order to show the existence of the nonanalyticity of the $\rho^{(2)}(\vartheta_{12})$ given by Eq.(2.2) at some small value of the relative angle $\vartheta_{12} = \vartheta_c$, consider the dependence of the integrand of Eq.(2.2) on the parent parton momentum K . The interplay between the decrease of the parent density R and the increase of the children densities $d^{(2)}$ with K produces a sharp maximum which is however ϑ_{12} dependent. The important element of running α_s analysis is that the position of this maximum is *independent of* Q_0 , since both distributions do not depend on Q_0 ². Now, for small relative angles the above maximum shifts *below* the lower limit Q_0/ϑ_{12} of the momentum integration. At that point the result changes nonanalytically (albeit very gently - analogously to the second order phase transitions in statistical systems). Namely, for ϑ_{12} bigger than ϑ_c , $\rho^{(2)}$ is given (to the exponential accuracy) by the Q_0 independent value of the integrand at the maximum. For ϑ_{12} below ϑ_c however, the result is given by the value of the integrand *at the lower bound* and obviously depends on Q_0 . Moreover, since $d_2(1) = 1$ in our exponential approximation, the density of pairs below ϑ_c is given entirely by the density of parent partons at the minimal momentum $K = Q_0/\vartheta_{12}$.

It is easy to verify explicitly the above considerations for constant α_s . In the logarithmic variables which are natural for this problem

$$Y = \ln(P\Theta/Q_0), \quad u = \ln(P\vartheta_{12}/Q_0), \quad v = \ln(\Theta/\vartheta_{12}), \quad (2.3)$$

$$\xi = \ln(P/K) = \ln(1/x), \quad (2.4)$$

the solution (2.2) reads

²Except of the overall normalization factor which does not influence the shape of the momentum dependence, hence is not relevant for the argument.

$$\rho^{(2)}(u, Y) = \int_0^u d\xi R(\xi, v) d_2(u - \xi). \quad (2.5)$$

Using the known momentum distribution of parent partons $\rho^{(1)}(\xi, Y) = \exp(2\gamma_0\sqrt{\xi(Y - \xi)})$ and replacing the vitality cut-off $Q_0 \rightarrow K\vartheta_{12}$, i.e. $Y \rightarrow v + \xi$, gives

$$\rho^{(2)}(u, Y) = \int_0^u \exp\left(\gamma_0(2\sqrt{\xi v} + n(u - \xi))\right) d\xi, \quad (2.6)$$

where we have also substituted the asymptotic form of the inhomogenous term $d_n(u - \xi) = \exp(n\gamma_0(u - \xi))$. The integer n , which for the two-body correlations is just 2, will be kept arbitrary in the following discussion. This allows for the direct generalization to the higher order correlations and multiplicity moments. The maximum of the integrand in (2.6) is located at

$$\xi_{max} = \frac{n^2}{v}. \quad (2.7)$$

This remains in the integration range only if

$$\tilde{\epsilon} < \frac{n^2}{n^2 + 1}, \quad (2.8)$$

where we have introduced the scaling variable

$$\tilde{\epsilon} = \frac{v}{u + v} = \frac{\ln(\Theta/\vartheta_{12})}{\ln(P\Theta/Q_0)}. \quad (2.9)$$

In this case the result for the density reads

$$\rho^{(2)}(u, Y) \sim \exp\left(\gamma_0\left(nu + \frac{v}{n}\right)\right), \quad (2.10)$$

and we obtain the power behaviour in the angle $\rho^{(2)} \sim \vartheta_{12}^{(3\gamma_0/2)}$. If $\xi_{max} > u$ the integral is saturated by the maximal value of the integrand at the boundary and we obtain

$$\rho^{(2)}(u, Y) \sim R(u, v) \sim \exp\left(2\gamma_0\sqrt{uv}\right), \quad \tilde{\epsilon} > \frac{n^2}{n^2 + 1}, \quad (2.11)$$

i.e. the two-parton distribution is given in terms of the single parton momentum distribution.

One can summarize our results in the "ε - scaling" form

$$\rho^{(2)}(\tilde{\epsilon}, Y) \sim \exp(\gamma_0 Y \tilde{\omega}(\tilde{\epsilon})), \quad (2.12)$$

$$\tilde{\omega}(\tilde{\epsilon}) = n - (n - \frac{1}{n})\tilde{\epsilon}, \quad \tilde{\epsilon} < \tilde{\epsilon}_c, \quad (2.13)$$

$$\tilde{\omega}(\tilde{\epsilon}) = 2\sqrt{\tilde{\epsilon}(1 - \tilde{\epsilon})}, \quad \tilde{\epsilon} > \tilde{\epsilon}_c. \quad (2.14)$$

where $\tilde{\epsilon}_c = n^2/(n^2 + 1)$. Note that the solution (2.14) is n -independent above $\tilde{\epsilon}_c$. The critical angle in Eq. (1.1) quoted in the Introduction corresponds to $\tilde{\epsilon}_c = 4/5$ for $n = 2$. It is always bigger than the minimal relative angle $\vartheta_{min} = Q_0/P$ and the maximal transverse momentum associated with ϑ_c grows like $(P/Q_0)^{1/5}$. The same result can be obtained from the exact solution for $\rho^{(2)}$ in terms of Bessel functions [2] which is valid also at finite energies.

The above solutions are displayed in Fig.1 for different n . The linear solutions for $\tilde{\epsilon} < \tilde{\epsilon}_c$ are tangent to the ellipse (2.14); at the critical point $\tilde{\epsilon}_c$ the functions $\tilde{\omega}(\tilde{\epsilon})$ and their derivatives are continuous but not their second derivative.

The same asymptotic result (2.12) for $\rho^{(2)}$ is also obtained from the nonlinear, first order differential equation

$$(\tilde{\omega} - \tilde{\epsilon}\tilde{\omega}')(\tilde{\omega} + (1 - \tilde{\epsilon})\tilde{\omega}') = 1 \quad (2.15)$$

which corresponds to Eq.(2.1) [3]. One finds the linear solution, Eq. (2.13), for any boundary value $\tilde{\omega}(0) = n > 0$ and the ellipse solution, Eq.(2.14), for the boundary value $\tilde{\omega}(1) = 0$. Eq. (2.15) can be solved explicitly for $\tilde{\omega}'$ with two roots in general; for a point on the ellipse there is only one root corresponding to a bifurcation point where the two solutions with proper boundary conditions at $\tilde{\epsilon} = 0$ and $\tilde{\epsilon} = 1$ meet.

The simpler case of fixed α_s or γ_0 considered above is instructive as it allows for the exact solution [2], in this case the dependence on the QCD scale Λ in Eq.(2.1) drops out and the only reference scale is provided by the cut-off Q_0 . The constant α_s solution is also obtained from the running α_s result when both β^2 and $\lambda = \ln Q_0/\Lambda \rightarrow \infty$ with their ratio $\beta^2/\lambda = \gamma_0^2$ fixed. This is equivalent to the famous limit $N_f \rightarrow 11N_c/2$ with $\Lambda \rightarrow 0$ tuned in such a way that the anomalous dimension γ_0 remains fixed. In other words Λ behaves as

$$\Lambda = Q_0 \exp\left(-\frac{12N_c}{\gamma_0^2(11N_c - 2N_f)}\right) \rightarrow 0, \quad (2.16)$$

in this limit.

III. RUNNING α_s AND DOUBLE SCALING

We employ the Mellin representation of the inclusive momentum distribution for running α_s , see Appendix B of Ref. [2] for the details. With the appropriate asymptotic forms of the energy moments one obtains

$$\rho^{(2)}(\vartheta_{12}, \Theta, P) \approx \int_{\gamma} \exp(sv) \mathcal{F}(s, L) \exp w_n(s, l) \frac{ds}{2\pi i}, \quad (3.1)$$

where

$$\mathcal{F}(s, x) = e^{\frac{\sigma}{2} g_-(s, x)} \exp \left[\frac{2\beta^2}{s} \ln \left(\frac{\sqrt{x}}{2\beta} g_+(s, x) \right) \right], \quad (3.2)$$

$$\exp w_n(s, l) = \int_{\lambda}^l d\sigma \exp v_n(s, \sigma), \quad (3.3)$$

$$v_n(s, \sigma) = -\frac{\sigma}{2} g_-(s, \sigma) - \frac{2\beta^2}{s} \ln \left(\frac{\sqrt{\sigma}}{2\beta} g_+(s, \sigma) \right) + 2n\beta\sqrt{\sigma},$$

$$g_{\pm}(s, x) = \sqrt{s^2 + 4\beta^2/x} \pm s, \quad (3.4)$$

and all prefactors have been neglected. The logarithmic variables are now defined with Λ as the reference scale

$$L = \ln(P\Theta/\Lambda), \quad l = \ln(P\vartheta_{12}/\Lambda), \quad \sigma = \ln(K\vartheta_{12}/\Lambda), \quad \lambda = \ln(Q_0/\Lambda), \quad (3.5)$$

and v as in Eq.(2.4). The saddle point of the σ integration is located at

$$\sigma^* = \frac{\beta^2(1-n^2)^2}{s^2 n^2}. \quad (3.6)$$

However the maximum of the σ integrand is not always within the bounds of the real σ integration. In particular for

$$s = s_{\odot} = -\frac{\beta}{\sqrt{\lambda}} \frac{n^2 - 1}{n}, \quad (3.7)$$

this maximum coincides with the lower cut-off at $\sigma = \lambda$. Second characteristic point in the complex s plane is the saddle point s_{\times} of the s integration. Depending on the external

parameters (e.g. ϑ_{12}) s_\times can be bigger or smaller than s_\odot thus determining the leading contribution to the integrand ³. The condition that the two points coincide determines the critical angle ϑ_c . In summary: for all ϑ_{12} the density of pairs can be written in the form

$$\rho^{(2)}(\epsilon, L, \rho) \sim \exp\left(2\beta\sqrt{L}(\omega_n(\epsilon, \rho) - 2\rho)\right), \quad (3.8)$$

with

$$\epsilon = \frac{v}{L} = \frac{\ln(\Theta/\vartheta_{12})}{\ln(P\Theta/\Lambda)}, \quad \rho = \sqrt{\lambda/L}. \quad (3.9)$$

For $\vartheta_{12} > \vartheta_c$ both integrations are done by the saddle point approximation with the result, $z = s\sqrt{L}/\beta$,

$$\omega_n(\epsilon) = \gamma(z(\epsilon)) + \epsilon z, \quad (3.10)$$

$$\gamma(z) = \frac{1}{2}(\sqrt{z^2 + 4} - z), \quad (3.11)$$

and $z_n(\epsilon)$ is the solution of the following algebraic equation

$$\gamma^2(z) - 2 \ln \gamma(z) - \epsilon z^2 = n^2 - 2 \ln n. \quad (3.12)$$

For $\vartheta_{12} < \vartheta_c$, one uses the value of the σ integrand at the lower boundary $\sigma = \lambda$ as the estimate for the σ integration which results in the different saddle point of the s integration.

The final result reads in this case

$$\omega_n(\epsilon, \rho) = \gamma(z) + \epsilon z - \rho(\gamma(z\rho) - n), \quad (3.13)$$

and $z_n(\epsilon, \rho)$ is determined by the different saddle point condition

$$\gamma^2(z) - 2 \ln \gamma(z) - \epsilon z^2 = \gamma^2(z\rho) - 2 \ln \gamma(z\rho). \quad (3.14)$$

The critical point

$$z_\odot = s_\odot\sqrt{L}/\beta = -\frac{n^2 - 1}{n\rho}, \quad (3.15)$$

³The value of s_\times is real.

coincides with the saddle point at $\vartheta_{12} = \vartheta_c$ or equivalently at $\epsilon = \epsilon_c$. This fact can be used to determine ϵ_c from e.g. Eqs.(3.12) and (3.15). The consistency check of such a procedure is the *equivalence* of both equations (3.12) and (3.14) at $z = z_\odot$. This is readily verified since $\gamma(z_\odot\rho) = n$. Our result for ϵ_c reads

$$\epsilon_c(\rho) = \frac{1}{z_\odot^2} \left(\gamma^2(z_\odot) - n^2 - \ln(\gamma^2(z_\odot)/n^2) \right). \quad (3.16)$$

or explicitly for $n = 2$ (see Fig.2)

$$\epsilon_c(\rho) = \frac{1}{4} \left(\sqrt{1 + \left(\frac{4\rho}{3}\right)^2 + 1} \right)^2 - \left(\frac{4\rho}{3}\right)^2 - \frac{1}{2} \left(\frac{4\rho}{3}\right)^2 \ln \left(\frac{3}{4\rho} \left(\sqrt{1 + \left(\frac{4\rho}{3}\right)^2 + 1} \right) / 2 \right). \quad (3.17)$$

Figure 3 shows the ω functions obtained from Eqs.(3.10 - 3.14) for few values of ρ . As expected from the general discussion in Sect.2, ϵ_c and $\omega_n(\epsilon, \rho)$ (for $\epsilon > \epsilon_c$) depend on Q_0 . This is in contrast to the constant α_s case, where the only scale was provided by Q_0 itself. For the running α_s , the second scale Λ allows to construct two dimensionless ratios relevant for this problem⁴, and, as a consequence, the simple ϵ scaling is violated for $\epsilon > \epsilon_c$ ($\vartheta_{12} < \vartheta_c$). On the other hand, $\omega_n(\epsilon, \rho)$ is independent of n for $\epsilon > \epsilon_c(n)$ as in the fixed α_s case.

It follows from Eq.(3.14) that the new solution, Eq.(3.13), has the correct behaviour at the kinematical boundary $\vartheta_{12} = Q_0/P$. One verifies readily that Eq.(3.14) has a real solution only for $\epsilon < \epsilon_{max} = 1 - \rho^2$ which corresponds to the above kinematic limit for ϑ_{12} . Around that point ω has the following expansion

$$\omega(\epsilon, \rho) \simeq 2\rho - 2 \ln(\rho) \sqrt{(\epsilon_{max} - \epsilon)} + A_3 \sqrt{(\epsilon_{max} - \epsilon)}^3 + \dots \quad (3.18)$$

with

$$A_3 = \frac{2\rho^2 \ln^{3/2}(1/\rho^2) - 2\rho^2 \ln(1/\rho^2) - (1 - \rho^2)(1 + 2\rho^2)}{2\rho^2 \ln^{3/2}(1/\rho^2)}. \quad (3.19)$$

This is to be contrasted with the asymptotic behaviour of the infinite energy limit $\omega(\epsilon)$ at $\epsilon \sim 1$ obtained from Eqs.(3.10-3.12).

⁴In the DLA the limit $\lambda \rightarrow \infty$ would lead to a divergence of the multiplicity and is therefore not allowed

$$\omega(\epsilon) \simeq \sqrt{(1-\epsilon) \ln \frac{1}{1-\epsilon}}. \quad (3.20)$$

The finite value of $\omega(\epsilon, \rho) = 2\rho$ at the boundary ensures our proper high energy normalization of the density $\rho^{(2)} \sim 1$ at $\vartheta_{12} = Q_0/P$. The coefficient $\ln(1/\rho^2)$ of the threshold behaviour turns into the additional logarithmic singularity of the asymptotic solution (3.20) around $\epsilon \sim 1$.

The constant α_s results of the previous Section can be recovered from Eq.(3.16) in the limit $\lambda \rightarrow \infty$ or $\rho \rightarrow 1$. One finds

$$\epsilon_c \simeq \frac{4}{5}(1 - \rho^2), \quad \rho \rightarrow 1, \quad (3.21)$$

which agrees with (2.14) since the scaling variable for the constant α_s , $\tilde{\epsilon} = \epsilon/(1 - \rho^2)$.

On the other hand in the high energy limit, $L \rightarrow \infty$, Q_0 – fixed, $\rho \rightarrow 0$ and Eq.(3.17) gives

$$\epsilon_c \simeq 1 - \frac{4\rho^2}{9} \ln\left(\frac{1}{\rho^2}\right), \quad \rho \rightarrow 0, \quad (3.22)$$

and the critical angle

$$\vartheta_c = \frac{\Lambda}{P} \exp(L(1 - \epsilon_c(\rho))), \quad (3.23)$$

may become small raising the question of the applicability of perturbative QCD in the new regime ($\vartheta_{12} < \vartheta_c$). However it is easy to show that the transverse momentum $P\vartheta_c$ is always bigger than the perturbative cut-off Q_0 which can be written as

$$Q_0 = \Lambda \exp(L\rho^2). \quad (3.24)$$

Since

$$\epsilon_c(\rho) < \epsilon_{max} = 1 - \rho^2 \quad (3.25)$$

is always in the physical region ($\vartheta_c > \vartheta_{12}^{min} = Q_0/P$), perturbative QCD applies also for $Q_0/P < \vartheta_{12} < \vartheta_c$. The above argument is valid only for $\rho > 0$. Exactly at $\rho = 0$ (infinite

energy, at fixed Q_0) the inequality (3.25) is saturated and using the asymptotic form (3.22) we obtain result (1.2) quoted in the Introduction. It implies the transverse momentum associated with ϑ_c grows as a power of the logarithm of P and is therefore larger than Q_0 .

At the critical angle the ω function, hence also $\rho^{(2)}$, are known analytically since the solution of the Eqs.(3.12,3.14), i.e. z_\odot , is known explicitly, c.f. Eq.(3.15). In particular in the high energy limit, Eq.(3.22), we obtain

$$\rho^{(2)}(\vartheta_c, P, \Theta) = \left(\frac{\ln(P\Theta/\Lambda)}{\lambda} \right)^{3\beta\sqrt{\lambda}}, \quad (3.26)$$

i.e. the density of pairs with the critical opening angle is growing only with a power of the logarithm of the energy.

The transition between the high energy and constant α_s limits can be conveniently presented in slightly different variables. In Fig.4 we show the function $\omega_R(\tilde{\epsilon}, \rho)$

$$\omega_R(\tilde{\epsilon}, \rho) = (\omega(\tilde{\epsilon}(1 - \rho^2), \rho) - 2\rho)/(1 - \rho), \quad (3.27)$$

as the function of $\tilde{\epsilon}$, in the normalized interval $0 < \tilde{\epsilon} < 1$, and for several values of ρ . The constant α_s regime (c.f. Fig.1) is already reached for $\rho \sim .8$

The limiting behaviour, Eq.(3.22) implies that the whole region $\vartheta_{12} < \vartheta_c$ shrinks to zero ($\epsilon = 1$) at infinite energy and constant Q_0 . Therefore the existence of the non-scaling part $\omega(\epsilon, \rho)$ can be regarded as the non-leading effect. However there is an important distinction between this type of finite energy corrections and the behaviour for $\vartheta_{12} > \vartheta_c$, namely below ϑ_c the leading contribution is Q_0 *dependent*, while above ϑ_c it is not. This follows from the general argument presented in Section 2. Second point is that precisely these corrections lead to the finite value of $\tilde{\epsilon}_c$ in the constant α_s limit. In other words, the high energy and constant α_s limits are not interchangeable at fixed Q_0 , and the region $\vartheta_{12} < \vartheta_c$ is responsible for the difference. With that point in mind, one can define the double scaling limit:

$$L \rightarrow \infty, \quad \epsilon, \rho - \text{fixed}. \quad (3.28)$$

In that limit $\omega(\epsilon, \rho)$ is the true asymptotic scaling function of two scaling variables, for all $0 < \epsilon, \rho < 1$. It is singular at $\epsilon = \epsilon_c(\rho)$ and becomes independent of ρ for $\epsilon < \epsilon_c(\rho)$. The

double scaling limit (3.28) requires Q_0 to grow with energy (L) according to Eq.(3.24). This is not quite along the standard assumption of constant Q_0 at high energies. However this limit allows us to make precise prediction in the $L \rightarrow \infty$ limit for the two regions above and below ϵ_c which are expected to persist for finite energies.

More importantly, comparison of Eqs.(3.23) and (3.24) shows that the necessary condition for applicability of the perturbative QCD, is now safely satisfied since the $P\vartheta_c$ grows exponentially faster than Q_0 due to (3.25). Therefore even the softer parents are described by the perturbative approach in this limit. The singularity nature of the ω function at $\epsilon_c(\rho)$ follows readily from Eqs.(3.10 - 3.14): $\omega(\epsilon, \rho)$ is continuous together with its ϵ derivative but the second derivative is not.

By changing ρ within $0 < \rho < 1$ one can move the bifurcation point ϵ_c through the whole range of $0 < \epsilon < 1$. Since at ϵ_c the ω function is known analytically and, moreover, the solution of the algebraic equations (3.12,3.14) is also known (c.f. Eq.(3.15)) we can provide the explicit analytic form for the scaling function in the parametric representation for all ϵ

$$\epsilon(t) = \frac{1}{4}(\sqrt{1+t^2} + 1)^2 - t^2 - \frac{t^2}{2} \ln \left(\frac{1}{2t}(\sqrt{1+t^2} + 1) \right) \quad (3.29)$$

$$\omega(t) = -\frac{2}{t}\epsilon(t) + \frac{1}{t}(\sqrt{1+t^2} + 1), \quad 0 < t < \frac{4}{3}. \quad (3.30)$$

For $0 < t < 4/3$ the asymptotic curve $\omega(\epsilon, \rho = 0)$ is produced. For finite non-zero ρ the representation (3.30) is valid for $4\rho/3 < t < 4/3$ and describes the ρ independent branch of the scaling function $\omega_n(\epsilon)$ for $\epsilon < \epsilon_c$.

IV. CONCLUSIONS AND PHENOMENOLOGICAL APPLICATIONS.

The angular correlation functions exhibit two kinematic regimes at high energies with quite different properties, separated by a critical angle ϑ_c or ϵ_c . Whereas for fixed α_s this critical behaviour occurs for fixed energy independent ϵ_c , in the realistic case of running α_s we find $\epsilon_c \rightarrow 1$ for $P \rightarrow \infty$. We consider here the preasymptotic region with $\epsilon_c < \epsilon_{max} < 1$

(for $Q_o/\Lambda > 1$) where besides the leading terms of the order $\ln \rho^{(2)} \sim \sqrt{L}$, the terms of all orders in $\sqrt{\lambda/L}$ are kept ($\lambda = \ln(Q_o/\Lambda)$, $L = \ln(P\Theta/\Lambda)$). Then the boundary conditions with finite ϵ_{max} can be fulfilled. The occurrence of the critical value ϵ_c is quite special to angular correlations and, for example, there is no such critical value in the distribution of the energy variable $\xi = \ln 1/x$ (the "hump backed plateau"): so, in case of fixed α_s , the function $\ln \rho^{(1)}(\xi)$ is asymptotically given by $\sqrt{\xi(Y - \xi)}$ in the full kinematic region whereas the angular correlation function is built up from the two different pieces in Eq.(2.14) with discontinuous second derivative.

In the following we want to point out two differences between the two regimes (in the theory with running α_s) with their phenomenological consequences.

1. Dependence of the cutoff Q_0 .

In the region $\epsilon < \epsilon_c$ the correlation function is Q_0 -independent and develops a scaling behaviour (ϵ -scaling [3]) whereas in the complementary region ($\epsilon > \epsilon_c$) this scaling is broken by Q_0). This leads to two possible effects:

a) as a function of energy the small ϵ region approaches the scaling limit which depends on the parameter Λ , but not on Q_0 , whereas at large ϵ the correlation function drops towards ϵ_{max} which depends in addition on the cutoff Q_0 with $\epsilon_{max} \rightarrow 1$ for $P \rightarrow \infty$, so it is nonscaling. This opens the possibility to determine independently the parameter Λ from the small ϵ data and the effective cutoff Q_0 from the large ϵ data. The first results from DELPHI [7] on " ϵ -scaling" could actually be interpreted along these lines: data with smaller $P\Theta$ drop down earlier with increasing ϵ . For more quantitative results an analysis with higher accuracy seems to be required: on the theoretical side an analysis beyond the DLA would be desirable and on the experimental side a better treatment of the jet axis problem, for example, by using the Energy-Multiplicity-Multiplicity observable [8,9];

b) another effect is the dependence of the correlations on the species of particles under the assumption that the particle mass acts as an effective transverse momentum cutoff and is therefore related to Q_0 [6]. The correlation functions for particles of different species (say

$\pi\pi$, KK , pp) should then be the same for small ϵ and different for large ϵ where $\rho^{(2)}$ for heavier particles vanishes for smaller ϵ_{max} .

2. Dependence of the correlation functions on their order n .

A convenient measure of correlations of higher order are the multiplicity moments, for example the factorial moments $f^{(q)} = \langle n(n-1)\dots(n-q+1) \rangle$ in a limited angular ring (dimension $D = 1$) or cone ($D = 2$) of half opening δ at polar angle ϑ to the primary parton (jet) direction [3–5]. These moments (usually one considers the normalised moments $F^{(q)} = f^{(q)} / \langle n \rangle^q$) behave at high energies like⁵

$$\ln F^{(n)} \sim 2\beta\sqrt{L}\omega_n(\epsilon, \rho). \quad (4.1)$$

One can determine the function $\omega_n(\epsilon, \rho)$ from the measurement of F_n after appropriate rescaling [3] (“ ω_n^F ”). Again for smaller ϵ one should obtain the predicted scaling limit $\omega_n(\epsilon, 0)$ whereas at sufficiently large $\epsilon > \epsilon_c(n)$ there is the dependence on $\rho = \sqrt{\lambda/L}$ but no dependence on the order n . This prediction follows as the opening angle δ determines the parent momentum $K > Q_0/\delta$ independent of the number of particles inside the cone because $d^{(n)} = 1$ at the threshold independently of n . In the same way one can extract $\omega_2^\rho(\epsilon, \rho)$ from $\rho^{(2)}$. Then all rescaled correlations should yield the same scaling function $\omega(\epsilon, \rho)$ independent of n for large ϵ

$$\omega_n^F \sim \omega_2^\rho. \quad (4.2)$$

Also in this region (large ϵ) the cutoff Q_0 could possibly be determined as lower limit of $K\delta$ or $K\vartheta_{12}$ where K is the momentum of the n -cluster or the pair considered.

We have discussed here the consequences of perturbative QCD in a preasymptotic region at high energies. At the energies realistic today one has to consider also finite energy effects. At high energies the width σ^2 of the peak in the variable ξ/Y of the integrand in Eqs.

⁵ Factorial $F^{(n)}$ or cumulant $C^{(n)}$ moments approach the same asymptotic limit but the nonleading corrections appear to be smaller for the $F^{(n)}$ [3,7].

(2.2,2.5) decreases like $1/\sqrt{L}$ and the two regimes become separated at ϵ_c . At finite energies there is an overlap between these regimes of this order. To illustrate the finite energy effects we show in Fig. 5 the rescaled normalized correlation function with the asymptotic behaviour [3]

$$\hat{r}(\epsilon) \equiv \frac{\ln r(\vartheta_{12})}{\sqrt{\ln P\Theta/\Lambda}} = 2\beta(\omega(\epsilon, 2) - 2\sqrt{1-\epsilon}) \quad (4.3)$$

and the exact numerical solution of the integral equation (2.1) for $\rho^{(2)}(\vartheta_{12})$ at LEP energies for different opening angles Θ . One can see that the scaling behaviour is approached quickly for $\epsilon < 0.4$ whereas for large ϵ the separation of curves is clearly visible. In comparison to our analytical calculations for finite λ/L (but still $L \rightarrow \infty$) the numerical results show in the central region a maximum of the correlation of lower height and position in ϵ . It should be noted, that the finite ϑ_c effects become more pronounced, hence easier to observe, at lower CM energies, for example at $\sqrt{s} = 5$ and 20 GeV we find $\epsilon_c = 0.65$ and $\epsilon_c = 0.75$ corresponding to $\vartheta_c = 10^\circ$ and $\vartheta_c = 2.5^\circ$ respectively.

In summary, the angular correlations – different from the case of the well studied energy distributions – show two regimes which are dominated either by the scaling behaviour of the well developed cascade or the hadronisation effects near the transverse momentum cutoff Q_o respectively with specific phenomenological consequences for both regions.

ACKNOWLEDGEMENTS

This work is supported in part by the KBN grants PB 2P03B19609 and PB 2P30225206.

APPENDIX A

In this Appendix we study in detail the analytic structure of the Mellin representation of the two-parton density $\rho^{(2)}$ in the constant α_s case. This serves as the basis of the generalization for the running α_s case performed Sect.III. The energy moments of the momentum distribution

$$\mu_n(Y) = P^{-n} \int_{Q_0/\Theta}^P k^n \rho^{(1)}(k, P, \Theta) dk = \int_0^Y e^{-ny} \rho^{(1)}(y, Y - y) dy, \quad (4.4)$$

read for constant α_s [9]

$$\begin{aligned} \mu_n(Y) = & \\ & \frac{1}{2\sqrt{n^2 + 4\gamma_0^2}} \left((\sqrt{n^2 + 4\gamma_0^2} + n) \exp\left[\frac{Y}{2}(\sqrt{n^2 + 4\gamma_0^2} - n)\right] \right. \\ & \left. + (\sqrt{n^2 + 4\gamma_0^2} - n) \exp\left[-\frac{Y}{2}(\sqrt{n^2 + 4\gamma_0^2} + n)\right] \right) \end{aligned} \quad (4.5)$$

The distribution of parent partons required in Eq.(2.2) can now be reconstructed as

$$R(y, x) = \int_{\gamma_1} \frac{ds}{2\pi i} e^{sx} \mu(s, x + v) \quad (4.6)$$

Therefore Eq.(2.2) can be rewritten in the form

$$\rho^{(2)}(\tilde{\epsilon}, Y) = e^{n\gamma_0 Y(1-\tilde{\epsilon})} \int_{\gamma} ds \exp\left(\frac{\tilde{\epsilon}Y}{2}(\sqrt{s^2 + \gamma_0^2} + s)\right) \quad (4.7)$$

$$\int_0^{Y(1-\tilde{\epsilon})} dy \exp\left(\frac{y}{2}(\sqrt{s^2 + \gamma_0^2} - s - 2n\gamma_0)\right) \quad (4.8)$$

where all preexponential factors have been omitted. The new contour γ follows from the change of variables $s \rightarrow -s$ and from the interchange of the s and y integrations. The integration over the parent momentum ($y = \ln(P/K)$) is now elementary and one is left with

$$\rho^{(2)}(\tilde{\epsilon}, Y) = \exp(n\gamma_0 Y(1-\tilde{\epsilon})) \int_{\gamma} \frac{ds}{2\pi i} \exp\left(\frac{\tilde{\epsilon}Y}{2}(\sqrt{s^2 + \gamma_0^2} + s)\right) \quad (4.9)$$

$$\exp\left(\frac{Y(1-\tilde{\epsilon})}{2}(\sqrt{s^2 + \gamma_0^2} - s - 2n\gamma_0)\right) \frac{1}{\sqrt{s^2 + \gamma_0^2} - s - 2n\gamma_0}, \quad (4.10)$$

where the nonleading contribution from the lower limit have been neglected. The final result is determined by the relative positions of the pole and the saddle point of the integrand. This analytical structure of is shown in Fig.6. The pole is located at

$$s_{\odot} = \gamma_0 \frac{1 - n^2}{n}, \quad (4.11)$$

while the saddle point position

$$s_{\times} = \gamma_0 \frac{1 - 2\tilde{\epsilon}}{\sqrt{\tilde{\epsilon}(1 - \tilde{\epsilon})}}, \quad (4.12)$$

depends on $\tilde{\epsilon}$, and the contour γ is now to the *left* of these singularities. For $\tilde{\epsilon} < \tilde{\epsilon}_c$ (Fig.6a) the saddle point is separated from the contour by the pole, and while deforming the contour $\gamma \rightarrow \gamma'$ one picks up the pole contribution (which is in fact dominating over the saddle contribution). This gives the result (2.12,2.13). For $\tilde{\epsilon} > \tilde{\epsilon}_c$ however $s_{\times} < s_{\odot}$ and the pole does not contribute, see Fig.6b. In this case the saddle point saturates the integral and one gets the n -independent result (2.14). Analogous structure occurs in the running α_s case as discussed in Sect. III.

REFERENCES

- [1] Yu. L. Dokshitzer, G. Marchesini, G. Oriani, *Nucl. Phys.* **B387** (1992) 675.
- [2] W. Ochs, J. Wosiek, *Phys. Lett.* **B289** (1992) 159.
- [3] W. Ochs, J. Wosiek, *Phys. Lett.* **B304** (1993) 144; *Zeit. Phys.* **C68** (1995) 269, see also preprint hep-ph/9412384.
- [4] Yu. L. Dokshitzer, I. Dremin, *Nucl. Phys.* **B402** (1993) 139.
- [5] Ph. Brax, J.L. Meunier, R. Peschanski, *Zeit. Phys.* **C62** (1994) 649.
- [6] Ya.I. Azimov, Yu.L. Dokshitzer, V.A. Khoze, S.I. Troyan, *Zeit. Phys.* **C27** (1985) 65; *Zeit. Phys.* **C31** (1961) 21.
- [7] F. Mandl, B. Buschbeck (DELPHI coll.), Proc. XXIV Int. Symp. on Multiparticle Dynamics, Vietri sul mare, 1994, Eds. A. Giovannini, S. Lupia, R. Ugoccioni, World Scientific, Singapore (1995) p.52.
- [8] Yu. Dokshitzer, V.A. Khoze, G. Marchesini, B.R. Webber, *Phys. Lett.* **B245** (1990) 243.
- [9] W. Ochs, J. Wosiek, Proc. Int. Europhysics Conf. on High Energy Physics, Brussels, July 1995, to be publ. by World Scientific, Singapore.

FIGURES

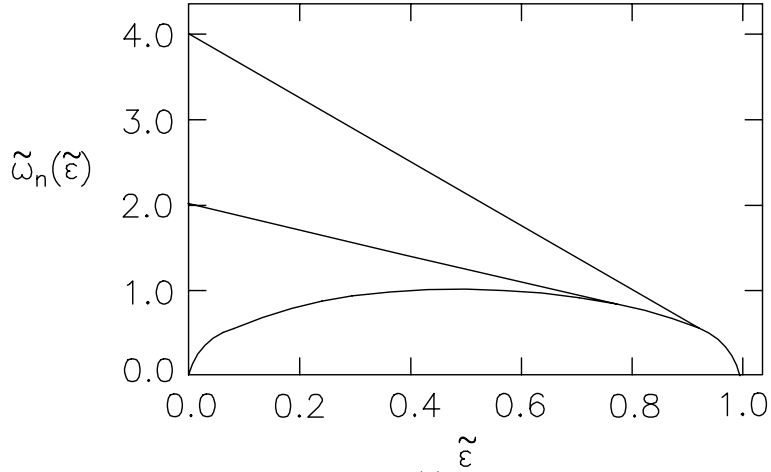


FIG. 1. Scaling function $\tilde{\omega}_n(\tilde{\epsilon})$ for fixed α_s . For $\tilde{\epsilon} < \tilde{\epsilon}_c$ two solutions corresponding to $n = 2$ and $n = 4$ are shown; for $\tilde{\epsilon} > \tilde{\epsilon}_c$ the solution is given by the ellipse for all n .

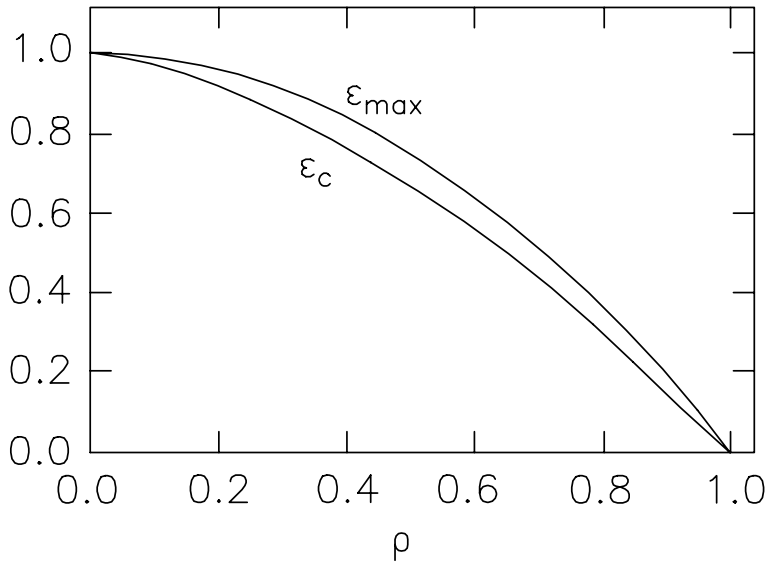


FIG. 2. Critical and the maximal values $\epsilon_c(\rho)$ and $\epsilon_{max}(\rho)$ as the function of ρ .

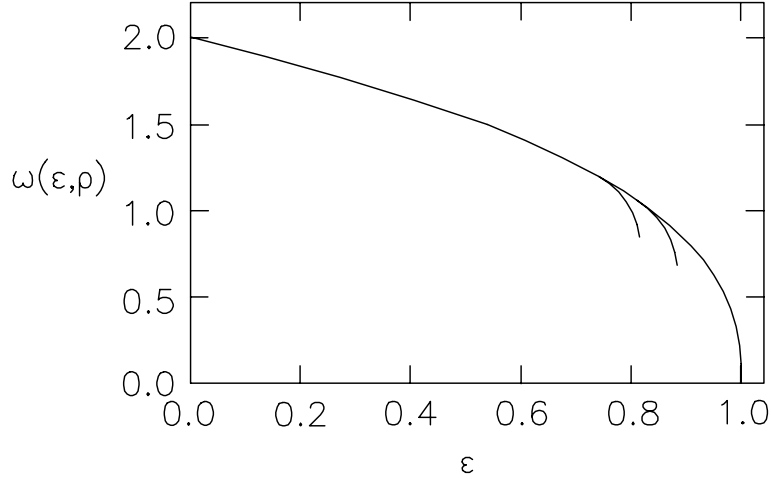


FIG. 3. Double scaling function $\omega_2(\epsilon, \rho)$. The rightmost curve corresponds to the asymptotic limit $\rho = 0$, the two branches are for $\rho = 0.35$ and $\rho = 0.43$ (from right to left).

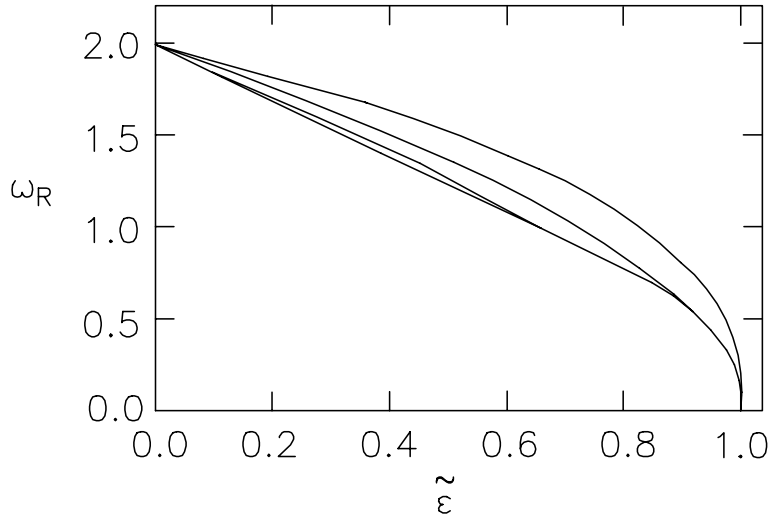


FIG. 4. Scaling plot of the function $\omega_R(\tilde{\epsilon}, \rho)$ of Eq.(3.27) in the $\tilde{\epsilon}$ variable for $\rho = 0.001, 0.4, 0.8, 0.999$ (from top to bottom); $\rho \sim 0$ corresponds to the running α_s , high energy limit, $\rho \sim 1$ to the constant α_s limit.

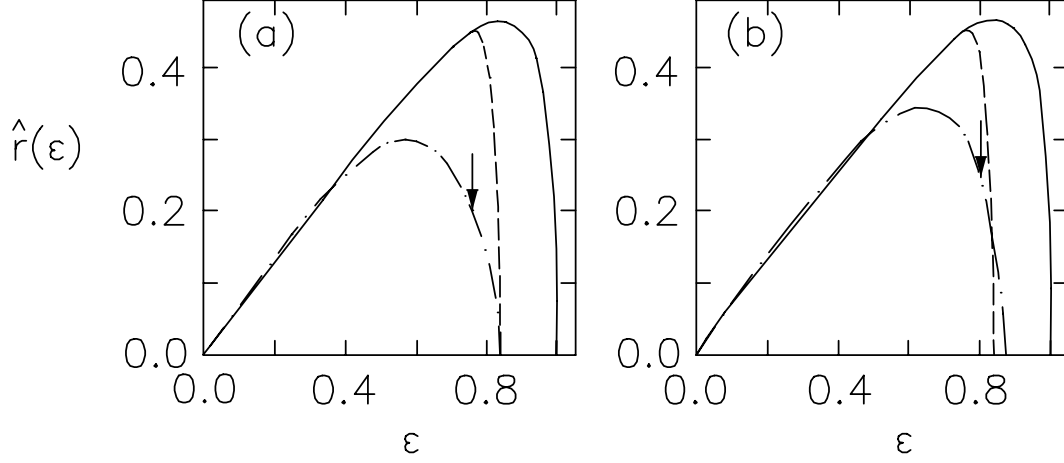


FIG. 5. Rescaled normalized correlation function $\hat{r}(\epsilon)$, c.f. Eq.(4.3) for asymptotic energies (full lines) and for LEP energies with jet opening angles (a) $\Theta = 15^\circ$ and (b) $\Theta = 60^\circ$. The dashed curves correspond to our asymptotic predictions of Eq.(3.12,3.14), the dash-dotted curves to the numerical solutions of Eq.(2.1) (for $\Lambda = 0.15$ GeV, $Q_0/\Lambda = 2$). The arrow indicates the position of the critical angle

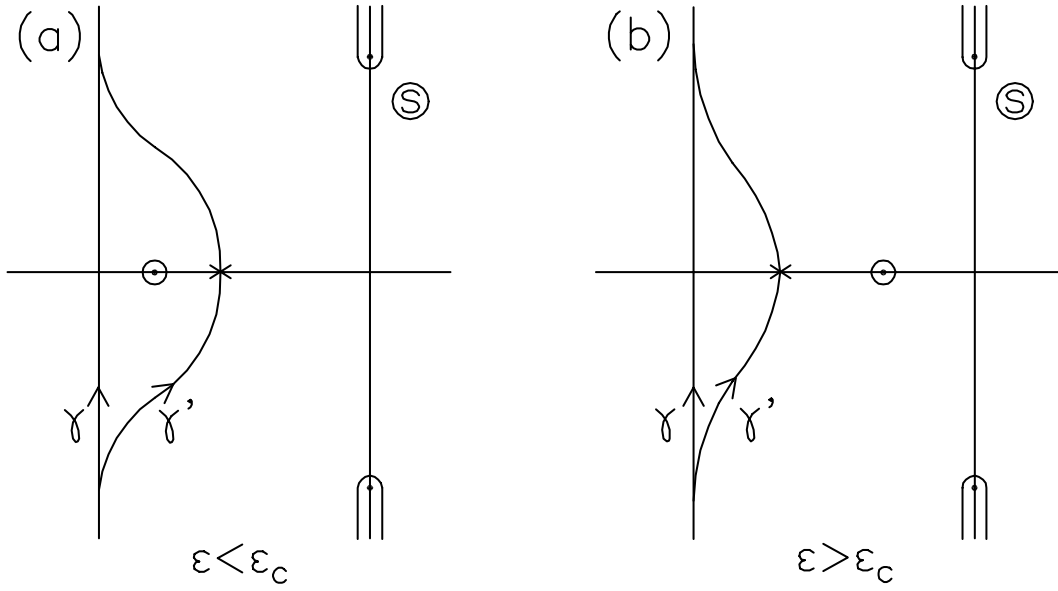


FIG. 6. Analytical structure of the Mellin representation Eq.(4.10) in the complex s plane; (a) $\epsilon < \epsilon_c$ and (b) $\epsilon > \epsilon_c$.